European Cells and Materials Vol. 24 2012 (pages 266-277) DOI: 10.22203/eCM.v024a19 ISSN 1473-2262

VASCULARISATION OF POROUS SCAFFOLDS IS IMPROVED BY INCORPORATION OF ADIPOSE TISSUE-DERIVED MICROVASCULAR FRAGMENTS

M.W. Laschke[1,2,*], S. Kleer[1,2], C. Scheuer[1,2], S. Schuler[1,2], P. Garcia[3], D. Eglin[4], M. Alini[4] and M.D. Menger[1,2]

[1]Institute for Clinical & Experimental Surgery, University of Saarland, 66421 Homburg/Saar, Germany
[2]Collaborative Research Partner Large Bone Defect Healing Program of AO Foundation
[3]Department of Trauma, Hand and Reconstructive Surgery, University of Saarland, 66421 Homburg/Saar, Germany
[4]AO Research Institute Davos, 7270 Davos Platz, Switzerland

Abstract

In tissue engineering, the generation of tissue constructs comprising preformed microvessels is a promising strategy to guarantee their adequate vascularisation after implantation. Herein, we analysed whether this may be achieved by seeding porous scaffolds with adipose tissue-derived microvascular fragments. Green fluorescent protein (GFP)-positive microvascular fragments were isolated by enzymatic digestion from epididymal fat pads of male C57BL/6-TgN(ACTB-EGFP)1Osb/J mice. Nano-size hydroxyapatite particles/poly(ester-urethane) scaffolds were seeded with these fragments and implanted into the dorsal skinfold chamber of C57BL/6 wild-type mice to study inosculation and vascularisation of the implants by means of intravital fluorescence microscopy, histology and immunohistochemistry over 2 weeks. Empty scaffolds served as controls. Vital microvascular fragments could be isolated from adipose tissue and seeded onto the scaffolds under dynamic pressure conditions. In the dorsal skinfold chamber, the fragments survived and exhibited a high angiogenic activity, resulting in the formation of GFP-positive microvascular networks within the implants. These networks developed interconnections to the host microvasculature, resulting in a significantly increased functional microvessel density at day 10 and 14 after implantation when compared to controls. Immunohistochemical analyses of vessel-seeded scaffolds revealed that >90 % of the microvessels in the implants' centre and ~60 % of microvessels in the surrounding host tissue were GFP-positive. This indicates that the scaffolds primarily vascularised by external inosculation. These novel findings demonstrate that the vascularisation of implanted porous scaffolds can be improved by incorporation of microvascular fragments. Accordingly, this approach may markedly contribute to the success of future tissue engineering applications in clinical practice.

Keywords: Tissue engineering; microvascular fragments; adipose tissue; inosculation; scaffold; polyurethane; vascularisation; angiogenesis.

*Address for correspondence:
Matthias W. Laschke, M.D., Ph.D.
Institute for Clinical & Experimental Surgery
University of Saarland
D-66421 Homburg/Saar
Germany

Telephone Number: +49 6841 162 6554
FAX Number: +49 6841 162 6553
E-mail: matthias.laschke@uks.eu

Introduction

The key challenge in tissue engineering is the establishment of clinically applicable strategies, which guarantee an adequate vascularisation and, thus, long-term survival and function of implanted tissue constructs (Laschke *et al.*, 2006; Bramfeldt *et al.*, 2010; Novosel *et al.*, 2011). In recent years, prevascularisation of tissue constructs has emerged as a promising concept to achieve this goal (Lokmic and Mitchell, 2008). In fact, the generation of a preformed microvascular network within a tissue construct prior to its implantation bears the major advantage that the network simply has to inosculate with the host microvasculature at the implantation site to get fully reperfused within a short period of time (Laschke *et al.*, 2009).

Basically, tissue constructs comprising preformed microvascular networks may be generated *in vitro* or *in situ*. For *in vitro* prevascularisation, scaffolds are seeded with different combinations of endothelial cells, mural cells and stem cells, which have the capacity to assemble to new microvessels when cultivated for several days to weeks (Koike *et al.*, 2004; Levenberg *et al.*, 2005; Shepherd *et al.*, 2006; Wang *et al.*, 2007). Accordingly, this approach involves complex and time-consuming cell isolation, seeding and cultivation procedures. Moreover, it does not necessarily result in the development of interconnected microvessels, which are organised in functional microvascular networks. To overcome this problem, scaffolds may be prevascularised *in situ*. For this purpose, they are implanted into a well vascularised host tissue of the body, such as subcutis (Laschke *et al.*, 2008a; Laschke *et al.*, 2010a; Laschke *et al.*, 2011a) or muscle (Kokemueller *et al.*, 2010). Subsequently, functional blood-perfused microvessels from the host tissue grow randomly into the implants by the process of angiogenesis. But, this is also associated with the invasion of the implants with unspecific granulation tissue. Alternatively, tissue constructs comprising a vascular pedicle can be generated by flap fabrication (Warnke *et al.*, 2006) or by implanting scaffolds into an isolation chamber containing an arteriovenous loop (Lokmic *et al.*, 2007; Beier *et al.*, 2010; Beier *et al.*, 2011). Finally, the *in situ* prevascularised constructs can be explanted and transferred into the defect site. However, all of these *in situ* approaches bear the disadvantage that they require three surgical interventions, i.e. the implantation of the scaffolds for prevascularisation, their removal and the final insertion into the host defect.

Therefore, the aim of the present study was to establish a novel method for the rapid prevascularisation of scaffolds, which may easily be used in the future under clinical conditions. For this purpose, we seeded poly(ester-

urethane) scaffolds with microvascular fragments. These fragments were freshly isolated from adipose tissue, which may also be harvested in large amounts under clinical conditions. Although this approach involved an enzymatic isolation procedure, we speculated based on previous findings of Shepherd *et al.* (2004, 2007) that these microvascular fragments survive and form functional microvascular networks in the porous scaffolds within a short period of time. To test this hypothesis, we implanted scaffolds seeded with microvascular fragments and non-seeded control scaffolds into mouse dorsal skinfold chambers and analysed their vascularisation potential by means of repetitive intravital fluorescence microscopy, histology and immunohistochemistry.

Materials and Methods

Animals

For our study we used 12- to 16-week-old transgenic C57BL/6-TgN(ACTB-EGFP)1Osb/J mice (The Jackson Laboratory, Bar Harbor, ME, USA) and corresponding C57BL/6 wild-type mice (Charles River, Sulzfeld, Germany) with a body weight of 22-26 g. During the experiments, the animals were housed one per cage and had free access to tap water and standard pellet food (Altromin, Lage, Germany). All experiments were approved by the local governmental animal care committee and were conducted in accordance with the German legislation on protection of animals and the NIH Guidelines for the Care and Use of Laboratory Animals (NIH Publication #85-23 Rev. 1985).

Isolation of microvascular fragments

Microvascular fragments were isolated from epididymal fat pads of male C57BL/6-TgN(ACTB-EGFP)1Osb/J donor mice. In these transgenic mice with an enhanced green fluorescent protein (EGFP) cDNA under the control of a chicken β-actin promoter and cytomegalovirus enhancer all of the tissues, with exception of erythrocytes and hair, exhibit a green fluorescence under blue-light excitation (Okabe *et al*., 1997). Accordingly, microvascular fragments could easily be detected by their GFP-positive signal after implantation into wild-type recipient animals.

The donor mice were anaesthetised by i.p. injection of ketamine (75 mg/kg body weight; Pharmacia GmbH, Erlangen, Germany) and xylazine 2 % (25 mg/kg body weight; Rompun; Bayer, Leverkusen, Germany). After midline laparotomy, the epididymal fat pads were harvested and transferred in 10 % Dulbecco's modified Eagle medium (DMEM; 100 U/mL penicillin, 0.1 mg/mL streptomycin; PAA, Cölbe, Germany). Then, the fat pads were washed three times in phosphate-buffered saline (PBS). They were finely minced with micro-scissors and digested in collagenase NB4G (0.5 U/mL; Serva, Heidelberg, Germany) for 5-7 min with vigorous stirring at 37 °C in a humidified atmosphere with 5 % CO_2. This resulted in the destruction of the fat cells. After neutralising the collagenase with PBS containing 20 % foetal calf serum (FCS), the cell suspension was incubated for 5 min at 37 °C and the fat supernatant was removed. The incubation period and removal of fat supernatants was repeated three to five times. The remaining cell suspension contained microvascular fragments, which were enriched in a small volume by centrifugation for 10 min at 40 g. Finally, the fragments were resuspended in PBS containing 20 % FCS to prevent their agglutination.

Viability testing of microvascular fragments

Apoptotic and necrotic cell death was analysed in small samples of microvascular fragments by fluorescence microscopy directly after the isolation procedure as well as after 1 h, 4 h and 24 h of cultivation in 10 % DMEM (PAA). For this purpose, the fragments were stained for 10 min with 2 µg/mL bisbenzimide (Sigma-Aldrich, Taufkirchen, Germany) to identify apoptotic cells with increased chromatin condensation and fragmentation and 2 µg/mL propidium iodide (Sigma-Aldrich) for the visualisation of necrotic cells. Subsequently, the microvascular fragments were examined by means of a BZ-8000 microscope (Keyence, Osaka, Japan).

Growth factor release of microvascular fragments

The amount of vascular endothelial growth factor (VEGF), basic fibroblast growth factor (bFGF) and platelet-derived growth factor-BB (PDGF-BB) released from cultivated microvascular fragments was measured in the culture medium by means of ELISA kits (VEGF, PDGF-BB: R&D Systems, Abingdon, UK; bFGF: RayBiotech, Norcross, GA, USA) using recombinant murine VEGF, bFGF and PDGF-BB as standards. For this purpose, microvascular fragments were isolated from 4 donor mice and cultivated for 72 h in 600 µL DMEM (10 % FCS, 100 U/mL penicillin, 0.1 mg/mL streptomycin; PAA) in a 48-well plate. Afterwards, 100 µL supernatant from each well were analysed by ELISA. Each sample was assayed in duplicate. The values were corrected to blank values (culture medium without incubated microvascular fragments).

Flow cytometric analysis of microvascular fragments

To evaluate, whether the microvascular fragments also contained mesenchymal stem cells or endothelial progenitor cells (EPCs), we additionally performed flow cytometric analyses. For this purpose, microvascular fragments from 4 donor mice were digested in accutase (PAA) for 30 min to single cells. Subsequently, the cells were analysed for the expression of the mesenchymal stem cell markers CD117-FITC and unlabelled rat-anti-mouse CD73, as well as the EPC markers Sca-1-FITC and VEGFR-2-PE (BD Pharmingen, Heidelberg, Germany). Isotype-identical rat IgG2aκ (BD Pharmingen) and goat-anti-rat IgG-Cy3 (Dianova GmbH, Hamburg, Germany) served as controls. Flow cytometric analyses were performed by means of a FACScan (BD Pharmingen). Data were evaluated by the software package CellQuest (BD Pharmingen).

Scaffold production and seeding

In the present study, we used porous nano-size hydroxyapatite particles/poly(ester-urethane) composite scaffolds with a size of ~3 x 3 x 1 mm, which have already been shown to exhibit an excellent *in vivo* biocompatibility (Laschke *et al.,* 2010b). The interconnected macropores of

the scaffolds had an average diameter of ~220 µm, which ideally promotes the ingrowth of new microvessels and granulation tissue at the implantation site (Druecke *et al.,* 2004; Laschke *et al*., 2010a; Laschke *et al*., 2011a). The elastomeric scaffolds were fabricated by a salt leaching-phase inverse process, as described previously in detail (Laschke *et al.*, 2010b).

The scaffolds were seeded with microvascular fragments, which were freshly isolated without an interim cultivation period. For this purpose, the scaffolds were fixed in the lumen of a modified 1 mL syringe (BD Plastipak; BD Biosciences, Heidelberg, Germany) by means of a rubber ring. The tip of the syringe was filled with 20 µL PBS containing the microvascular fragments. Subsequently, negative and positive pressure was alternately induced three to five times in the syringe so that the microvascular fragments could pass the scaffolds from both sides and were finally trapped in the scaffold pores. After the seeding procedure, the scaffolds were carefully taken out of the syringe and embedded for histological analyses or directly transferred into dorsal skinfold chambers for further *in vivo* experiments.

Dorsal skinfold chamber model

Scaffolds seeded with microvascular fragments and non-seeded control scaffolds were implanted into dorsal skinfold chambers of C57BL/6 wild-type mice for the in vivo analysis of their vascularisation by means of intravital fluorescence microscopy. For the preparation of the chamber, the animals were anaesthetised by i.p. injection of ketamine (75 mg/kg body weight; Pharmacia GmbH) and xylazine 2 % (25 mg/kg body weight; Rompun). The preparation procedure has been described previously in detail (Laschke *et al*., 2011b). After the preparation, the animals were allowed to recover for 48 h in order to exclude deterioration of the microcirculation due to the anaesthesia and the surgical trauma. Subsequently, the cover glass of the dorsal skinfold chamber was temporarily removed and the scaffolds were placed onto the striated muscle tissue within the centre of each chamber, taking care to avoid contamination, mechanical irritation or damage of the tissue.

Intravital fluorescence microscopy and microcirculatory analysis

For intravital fluorescence microscopy, the animals were anaesthetised by i.p. injection of ketamine (75 mg/kg body weight; Pharmacia GmbH) and xylazine 2 % (25 mg/kg body weight; Rompun). Subsequently, 0.05 mL 5 % fluorescein isothiocyanate (FITC)-labelled dextran 150,000 (Sigma-Aldrich) was given i.v. via the retrobulbary space for contrast enhancement of the perfused microvasculature by staining of blood plasma. The dorsal skinfold chamber was attached to the microscopic stage. Microscopy was performed using a Zeiss Axiotech microscope (Zeiss, Oberkochen, Germany) with a 100 W mercury lamp attached to an epi-illumination filter block for blue, green and ultraviolet light. The microscopic images were recorded by a charge-coupled device video camera (FK6990, Pieper, Schwerte, Germany) and transferred to a DVD system for off-line evaluation. By means of 5x, 10x and 20x long-distance objectives (Zeiss) magnifications of x115, x230 and x460 were achieved on a 14 inch video screen (KV-14CT1E, Sony, Tokyo, Japan).

Quantitative off-line analysis of the microscopic images was performed using the software package CapImage (Zeintl, Heidelberg, Germany). Vascularisation of the scaffolds was analysed at a magnification of x460 in 8 different microvascular regions of interest (ROIs) in the border zone and 8 different microvascular ROIs in central surface areas of the implants. The ROIs exhibited a size of 0.4 mm². To guarantee that identical standard locations for ROIs were visualised at each observation time point, images of ROIs were printed out with a video printer (UP-895CE; Sony) during the first microscopy, i.e. directly after scaffold implantation into the dorsal skinfold chamber. These ROIs were then repetitively analysed during a 14-day observation period. Perfused ROIs (given in % of all analysed ROIs) were defined as areas that exhibited either newly developed red blood cell (RBC)-perfused microvessels or reperfused microvascular fragments. In addition, the functional microvessel density, i.e. the length of all RBC-perfused blood vessels per ROI, was measured and is given in cm/cm².

Experimental protocol

In a first set of experiments, microvascular fragments were isolated by enzymatic digestion from epididymal fat pads of 6 male TgN(ACTB-EGFP)1Osb/J mice and seeded onto 6 porous nano-size hydroxyapatite particles/poly(ester-urethane) composite scaffolds (1 donor per scaffold). Directly after the seeding procedure, the scaffolds were prepared for histological analyses of the fragments' distribution and density within the constructs.

To analyse the vascularisation of the scaffolds *in vivo*, microvascular fragments from 8 male TgN(ACTB-EGFP)1Osb/J mice were seeded onto 8 scaffolds (1 donor per scaffold). The 8 scaffolds and 7 non-seeded control scaffolds were then implanted into the dorsal skinfold chamber of 15 C57BL/6 wild-type mice. According to the seeded scaffolds, non-seeded control scaffolds were also flushed with PBS before implantation. Intravital fluorescence microscopy of the scaffolds' vascularisation was performed immediately as well as 3, 6, 10 and 14 d after implantation. At the end of the in vivo experiments, the animals were sacrificed with an overdose of the anaesthetic and the dorsal skinfold preparations were excised for further histological and immunohistochemical analyses.

Histology and immunohistochemistry

For light microscopy, formalin-fixed specimens of scaffolds seeded with microvascular fragments or dorsal skinfold preparations were embedded in paraffin. Three-µm-thick sections were cut and stained with haematoxylin and eosin according to standard procedures. For the quantitative analysis of the density of microvascular fragments in freshly seeded scaffolds (given in mm^{-2}), sections were analysed by means of a BZ-8000 microscopic system (Keyence).

For immunohistochemical detection of GFP-positive and -negative microvessels in the border and centre

of implanted scaffolds, paraffin-embedded 3 µm-thick sections were stained with a monoclonal rat-anti-mouse antibody against CD31 (1:30; Dianova) to detect endothelial cells and with a goat-anti-GFP antibody (1:200; Biomol, Hamburg, Germany) to enhance GFP-fluorescence. As secondary antibodies a goat-anti-rat Cy3 antibody (1:50; Dianova) and a biotin-labelled donkey-anti-goat antibody (1:15; Jackson ImmunoResearch, Baltimore, MD, USA), which was detected by fluorescein labelled-streptavidin (1:50; Vector Labs, Burlingame, CA, USA), were used. For this purpose, the sections were placed in Coplin jars with 0.05 % citraconic anhydride solution (pH 7.4) for 1 h at 98 °C and then incubated overnight at 4 °C with the first antibody, followed by the appropriate secondary antibody at 37 °C for 2 h. On each section, cell nuclei were stained with Hoechst (1:500; Sigma-Aldrich) to merge the images exactly. For the quantitative analysis of the density (given in mm^{-2}) and the fraction of GFP-positive and -negative microvessels (given in %) in the border and centre of the implants, the sections were examined using a BX60 microscope (Olympus, Hamburg, Germany). The identical staining protocol was used for scaffolds that were not implanted into the dorsal skinfold chamber, but directly analysed after the seeding procedure.

In addition, vessel-seeded scaffolds were stained with a monoclonal rat-anti-mouse antibody against CD31 (1:30; Dianova) to detect endothelial cells and with a monoclonal mouse-anti-α-smooth muscle actin (SMA) antibody for the visualisation of perivascular mural cell coverage (1:50; Sigma-Aldrich). As secondary antibodies a goat-anti-rat Cy3 antibody (1:50; Dianova) and a goat-anti-mouse Alexa488 antibody (1:200; Molecular Probes, Eugene, OR, USA) were used. On each section, cell nuclei were stained with Hoechst (1:500; Sigma-Aldrich) to merge the images exactly.

Detection of myeloperoxidase (MPO)-positive neutrophils and F4/80-positive macrophages in the newly formed granulation tissue invading the implants was performed by avidin-biotin complex immunohistochemistry. For this purpose, a polyclonal rabbit anti-MPO antibody (0.01 mg/mL, ready to use; Abcam, Cambridge, UK) and a monoclonal rat anti-F4/80 antibody (1:50; Abcam) served as primary antibodies followed by a goat-anti-rabbit IgG biotin antibody (ready to use; Abcam) and a goat-anti-rat IgG biotin antibody (1:50; Dianova) as secondary antibodies, which were then incubated with peroxidase-labelled avidin (1:50; Sigma-Aldrich). 3,3' diaminobenzidine (Sigma-Aldrich) was used as chromogen. The sections were counterstained with Mayer's hemalaun (Merck, Darmstadt, Germany) and the amount of neutrophils and macrophages within the granulation tissue (given in % of all cells in 10 high-power fields) was quantitatively assessed using the BX60 microscope (Olympus).

Statistics

After testing the data for normal distribution and equal variance, differences between two groups were analysed by the unpaired Student's *t*-test. To test for time effects in the individual groups, ANOVA for repeated measures was applied. This was followed by the Student-Newman-Keuls test including the correction of the alpha error according to Bonferroni probabilities to compensate for multiple comparisons (SigmaStat; Jandel Corporation; San Rafael, CA, USA). All values are expressed as means ± SEM. Statistical significance was accepted for a value of $p < 0.05$.

Results

Isolation and viability of microvascular fragments

The entire isolation of microvascular fragments from epididymal fat pads of C57BL/6-TgN(ACTB-EGFP)1Osb/J donor mice did not take longer than ~2 h. From one donor mouse, we could isolate ~600 microvascular fragments. The average length of these fragments was 154 ±13 µm. Fluorescence microscopy of bisbenzimide/propidium iodide-stained fragments directly after the isolation, as well as during a 24 h cultivation period, revealed that the procedure did not markedly affect the viability of the fragments (Figs. 1a and b). They neither contained relevant numbers of apoptotic nor necrotic cells.

Growth factor release and stem cell content of microvascular fragments

In a subset of experiments, we investigated by ELISA, whether isolated microvascular fragments are capable of promoting angiogenesis by the production and release of pro-angiogenic growth factors. Of interest, we found that microvascular fragments, which were cultivated for 72 h, released 30 ±6 pg/mL VEGF and 679 ±58 pg/mL bFGF, but not PDGF-BB, into the culture medium.

Additional flow cytometric analyses of microvascular fragments revealed that they contained 21 ±1 % and 5 ±1 % of cells, which expressed the mesenchymal stem cell markers CD73 and CD117, respectively. Moreover, they contained 5 ±1 % Sca-1/VEGFR-2-positive EPCs.

Seeding of scaffolds with microvascular fragments

In a first attempt, static seeding of porous scaffolds with microvascular fragments was performed by pipetting PBS containing microvascular fragments on top of the implants. By this, almost all fragments stuck to the scaffolds' surface and did not penetrate through the pores into the centre. Therefore, we established a dynamic seeding procedure during which negative and positive pressure was alternately induced in the scaffold pores. Histological analyses showed that in this case several fragments were again localised on the scaffolds' surface (Figs. 1c and d). However, many fragments could also be detected in the centre pores (Figs. 1c and e), indicating that this type of seeding markedly improved their distribution within the implants. The density of the fragments was 5.8 ±0.4 mm^{-2}. As expected, endothelial cells inside the fragments were double positive for CD31 and GFP (Figs. 1f-h). In addition, we found that the microvascular fragments exhibited a stabilising layer of α-SMA-positive mural cells, which is in line with the fact that they were harvested from the mature microvasculature of fat tissue (Figs. 1i-k).

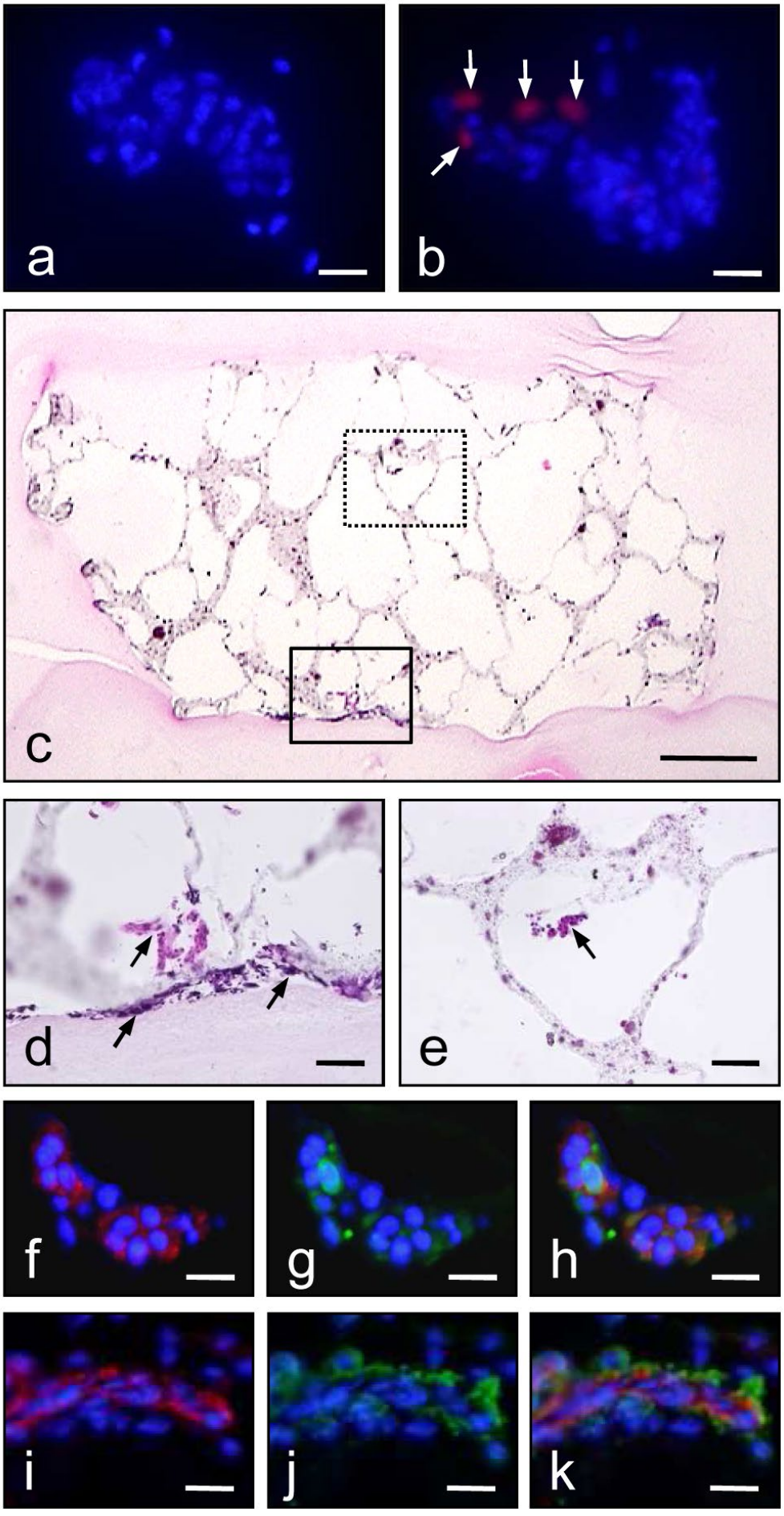

Fig. 1. a, b: Multi-fluorescence microscopy of microvascular fragments directly after the isolation procedure (a) and after 24 h of cultivation in DMEM (b). The fragments were stained with bisbenzimide (a, b, blue) for the detection of apoptotic cells and propidium iodide for the visualisation of necrotic cells (a, b, red). Note that the fragments do not contain any apoptotic cells with an increased chromatin condensation and fragmentation. The cultivated fragment exhibits only a few necrotic cells (b, arrows). **c-e:** Haematoxylin-eosin stained cross sections of a porous scaffold seeded with microvascular fragments (d, e, arrows). d and e display higher magnifications of the border (closed line) and the centre (dotted line) of the scaffold in c. **f-k:** Immunohistochemical characterisation of microvascular fragments within a scaffold pore. Histological sections were stained with bisbenzimide to identify cell nuclei (f-k, blue), an antibody against CD31 for the detection of endothelial cells (f, i, red), an antibody against GFP (g, green) and an antibody against α-SMA (j, green). h and k display merges of f, g and i, j, respectively. Scale bars: a, b = 18 µm; c = 370 µm; d, e = 55 µm; f-k = 16 µm.

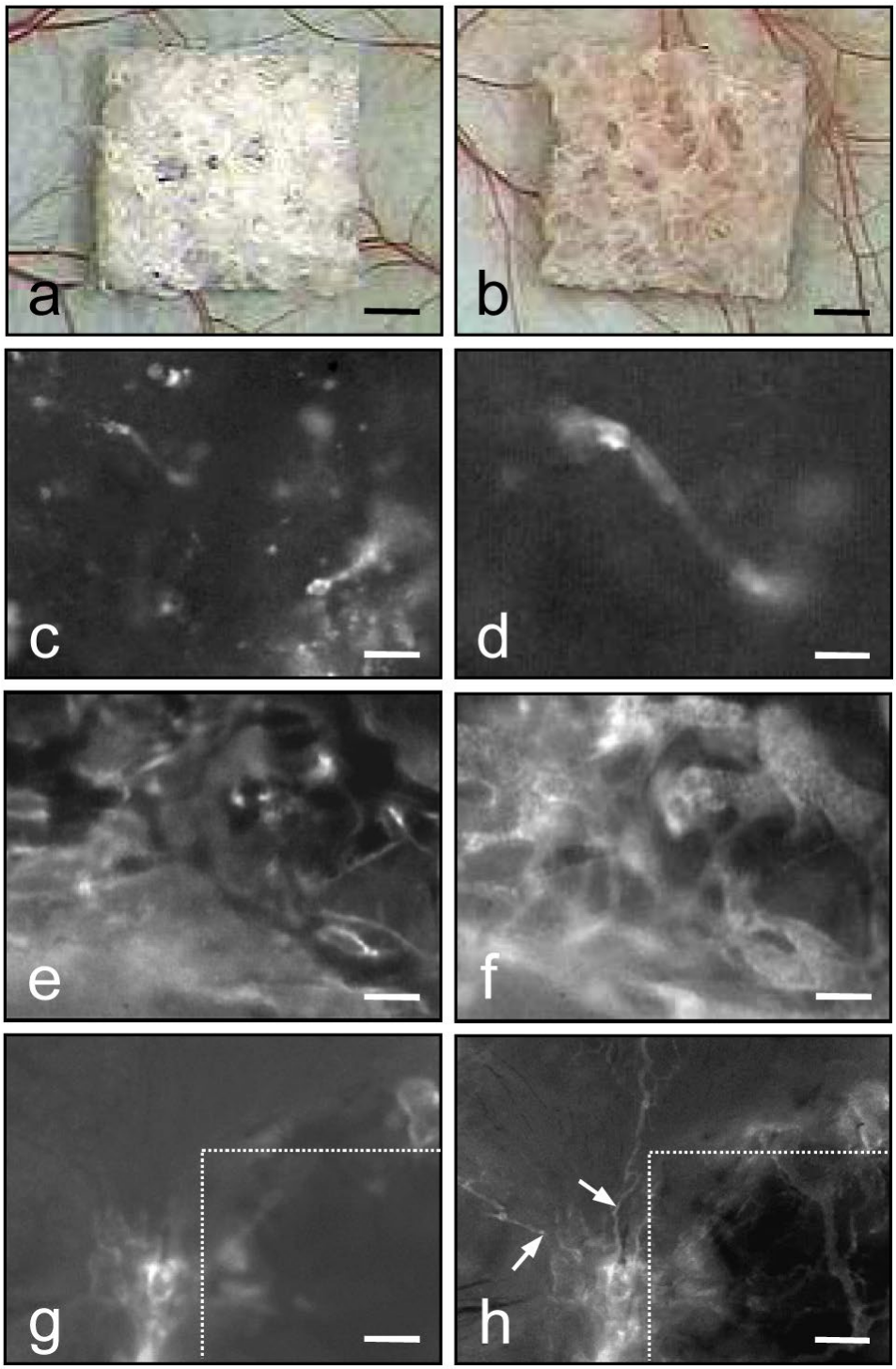

Fig. 2. a, b: Stereo microscopy of a non-seeded control scaffold (a) and a scaffold seeded with microvascular fragments (b) directly after implantation into the dorsal skinfold chamber of C57BL/6 wild-type mice. Note that the seeded scaffold appears reddish due to residual red blood cells inside the scaffold pores, because the donor mice were not perfused with PBS before harvesting the microvascular fragments from the fat tissue. **c-h:** Intravital fluorescence microscopy of a scaffold seeded with microvascular fragments directly (c, d) as well as at day 14 (e-h) after implantation. Initially, the GFP-positive microvascular fragments can easily be visualised in blue-light epi-illumination (c, higher magnification in d) on the scaffold surface, which is averted from the underlying host tissue. After 14 d, these fragments have developed into a dense microvascular network with a GFP-positive endothelium (e). Blood perfusion of this network is proven by injection of the plasma marker 5 % FITC-labelled dextran 150,000 in blue-light epi-illumination (f, compare with identical microscopic region of interest in e) and results from interconnections of GFP-positive microvessels to the GFP-negative microvessels of the host tissue. These interconnections (h, arrows) can be directly identified by comparing identical microscopic regions of interest before (g, only detection of GFP signal) and after injection of 5 % FITC-labelled dextran 150,000 (h, detection of all blood vessels) in the border zone of the scaffold (marked by dotted line). Scale bars: a, b = 650 µm; c = 75 µm; d = 25 µm; e, f = 50 µm; g, h = 200 µm.

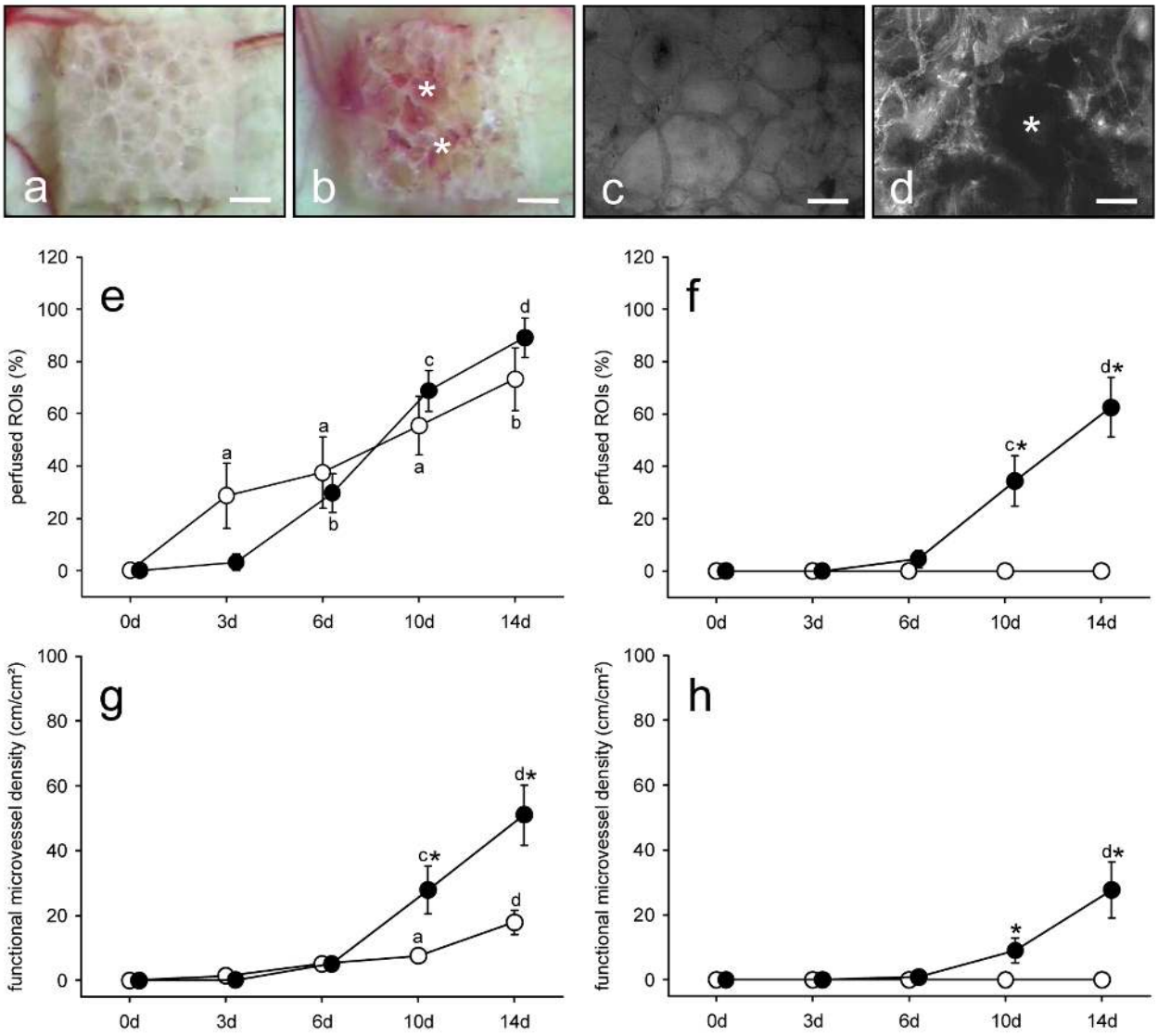

Fig. 3. a-d: Stereo microscopy (a, b) and intravital fluorescence microscopy in blue-light epi-illumination with contrast enhancement by 5 % FITC-labelled dextran 150,000 i.v. (c, d) of the surface of a non-seeded control scaffold (a, c) and a scaffold seeded with microvascular fragments (b, d) at day 14 after implantation into the dorsal skinfold chamber. Note that the seeded scaffold exhibits a markedly improved vascularisation when compared to the control scaffold. This is associated with the formation of haemorrhages (asterisks) inside the implant (b, d). Scale bars: a, b = 700 μm; c, d = 400 μm. **e-h:** Perfused regions of interest (ROIs) (in % of all analysed ROIs exhibiting an individual size of 0.4 mm²) (e, f) and functional microvessel density (cm/cm²) (g, h) within the border (e, g) and central surface areas (f, h) of non-seeded control (white circles; $n = 7$) and seeded scaffolds (black circles; $n = 8$) after implantation into dorsal skinfold chambers, as assessed by intravital fluorescence microscopy and computer-assisted image analysis. Means ± SEM. $^{a}p < 0.05$ *vs*. 0 d within each individual group; $^{b}p < 0.05$ *vs*. 0 d and 3 d within each individual group; $^{c}p < 0.05$ *vs*. 0 d, 3 d and 6 d within each individual group; $^{d}p < 0.05$ *vs*. 0 d, 3 d, 6 d and 10 d within each individual group; $*p < 0.05$ *vs*. control.

Vascularisation of implanted scaffolds

Because the donor mice were not perfused with PBS before harvesting the microvascular fragments from the fat tissue, the seeded scaffolds appeared reddish directly after the implantation into the dorsal skinfold chamber of C57BL/6 wild-type mice (Figs. 2a and b). The microvascular fragments could easily be visualised on the scaffolds' surface by means of intravital fluorescence microscopy due to their GFP-positive signal (Figs. 2c and d). During the following days, the fragments started to proliferate and interconnect with each other to form dense microvascular networks within the implants, which still exhibited a GFP-positive endothelium (Fig. 2e). Blood perfusion of these networks was proven by injection of the plasma marker 5 % FITC-labelled dextran 150,000 (Fig. 2f) and resulted from the development of interconnections to the host microvasculature during the 14-day observation period by the process of inosculation (Figs. 2g and h).

The comparison of scaffolds seeded with microvascular fragments and non-seeded control scaffolds revealed

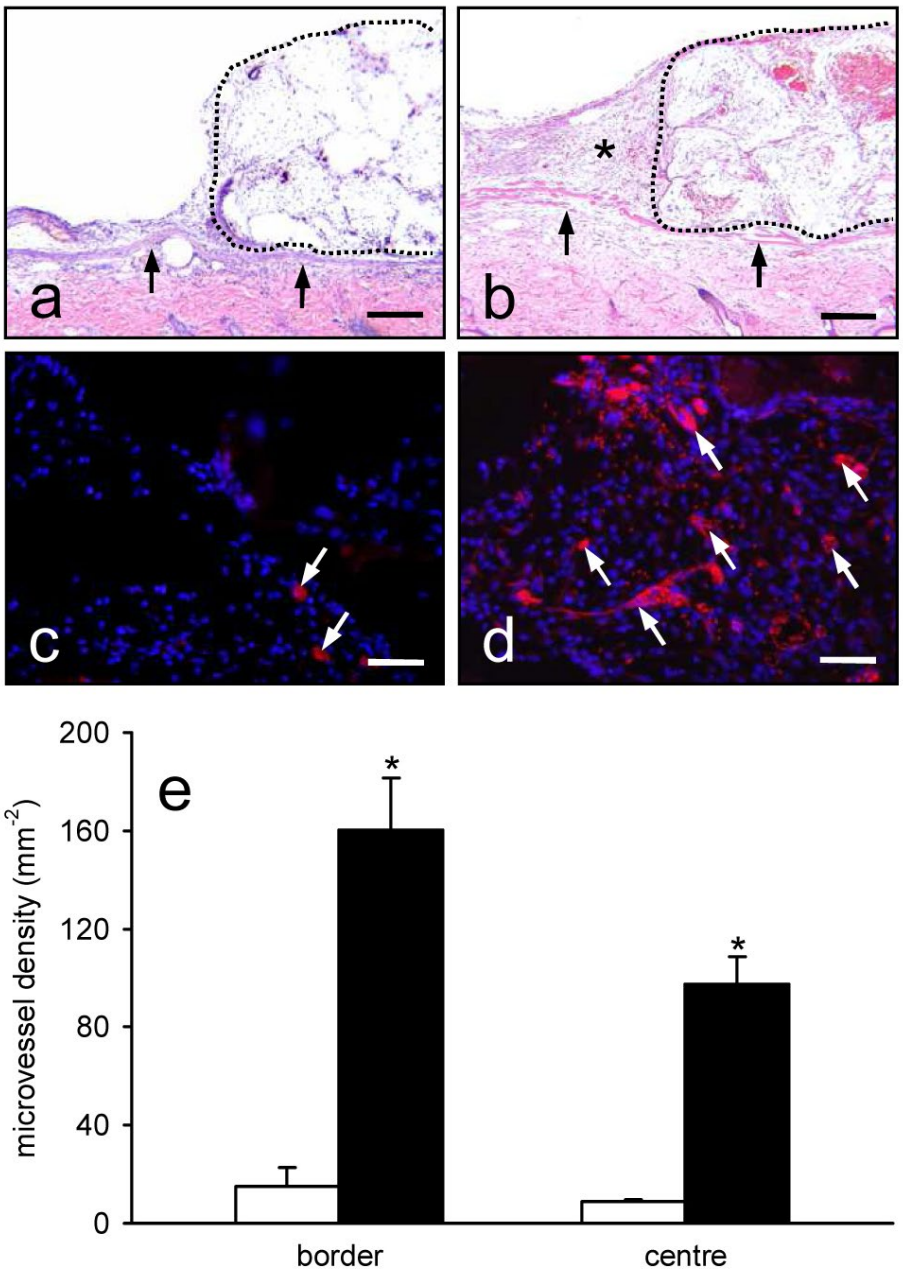

Fig. 4. a, b: Haematoxylin-eosin stained cross sections of a non-seeded control scaffold (a, borders marked by dotted line) and a scaffold seeded with microvascular fragments (b, borders marked by dotted line) at day 14 after implantation onto the host striated muscle tissue (arrows) within the dorsal skinfold chamber. Note that in contrast to the control, the seeded scaffold is well incorporated into a newly formed granulation tissue (b, asterisk). **c, d:** Immunohistochemical detection of CD31-positive microvessels (arrows) in the centre of a control (c) and a seeded scaffold (d) at day 14. The sections were additionally stained with bisbenzimide to identify cell nuclei. Scale bars: a, b = 230 µm; c, d = 70 µm. **e:** Microvessel density (mm^{-2}) within the border and centre of control (white bars; $n = 7$) and seeded scaffolds (black bars; $n = 8$) at day 14 after implantation into dorsal skinfold chambers. Means ± SEM. *$p < 0.05$ *vs*. control.

that both implant types induced an angiogenic host tissue response in the dorsal skinfold chamber with the formation of new microvessels at the implants' border zones beginning at day 3 (Fig. 3e). However, during the further time course of the experiment the seeded scaffolds exhibited a markedly improved vascularisation, as indicated by a significantly increased functional microvessel density of the border zones between day 10 and 14 when compared to controls (Figs. 3a, b and g). Moreover, a progressively increasing number of perfused microvessels could be detected in central surface areas of scaffolds seeded with microvascular fragments from day 6 onwards, whereas non-seeded control scaffolds completely lacked a central blood perfusion (Figs. 3c, d, f and h). The improved vascularisation of seeded scaffolds was associated with the formation of haemorrhages inside the implants (Figs. 3b and d).

Incorporation and angioarchitecture of implanted scaffolds

Histological examination of the scaffolds at day 14 after implantation into the dorsal skinfold chamber revealed that scaffolds seeded with microvascular fragments were better incorporated into the surrounding host tissue when compared to controls, as indicated by the formation of a prominent granulation tissue in the border zones of the implants (Figs. 4a and b). Of interest, this was not caused by a stronger immune response. In fact, the granulation tissue invading the scaffolds of both groups revealed comparable amounts of infiltrating MPO-positive neutrophils (vessel-seeded scaffolds: 12 ±1 % *vs*. non-seeded scaffolds: 13 ±2 %; $p > 0.05$) and F4/80-positive macrophages (vessel-seeded scaffolds: 8 ±1 % *vs*. non-seeded scaffolds: 10 ±1 %; $p > 0.05$). Accordingly, the seeding of scaffolds with microvascular fragments did not

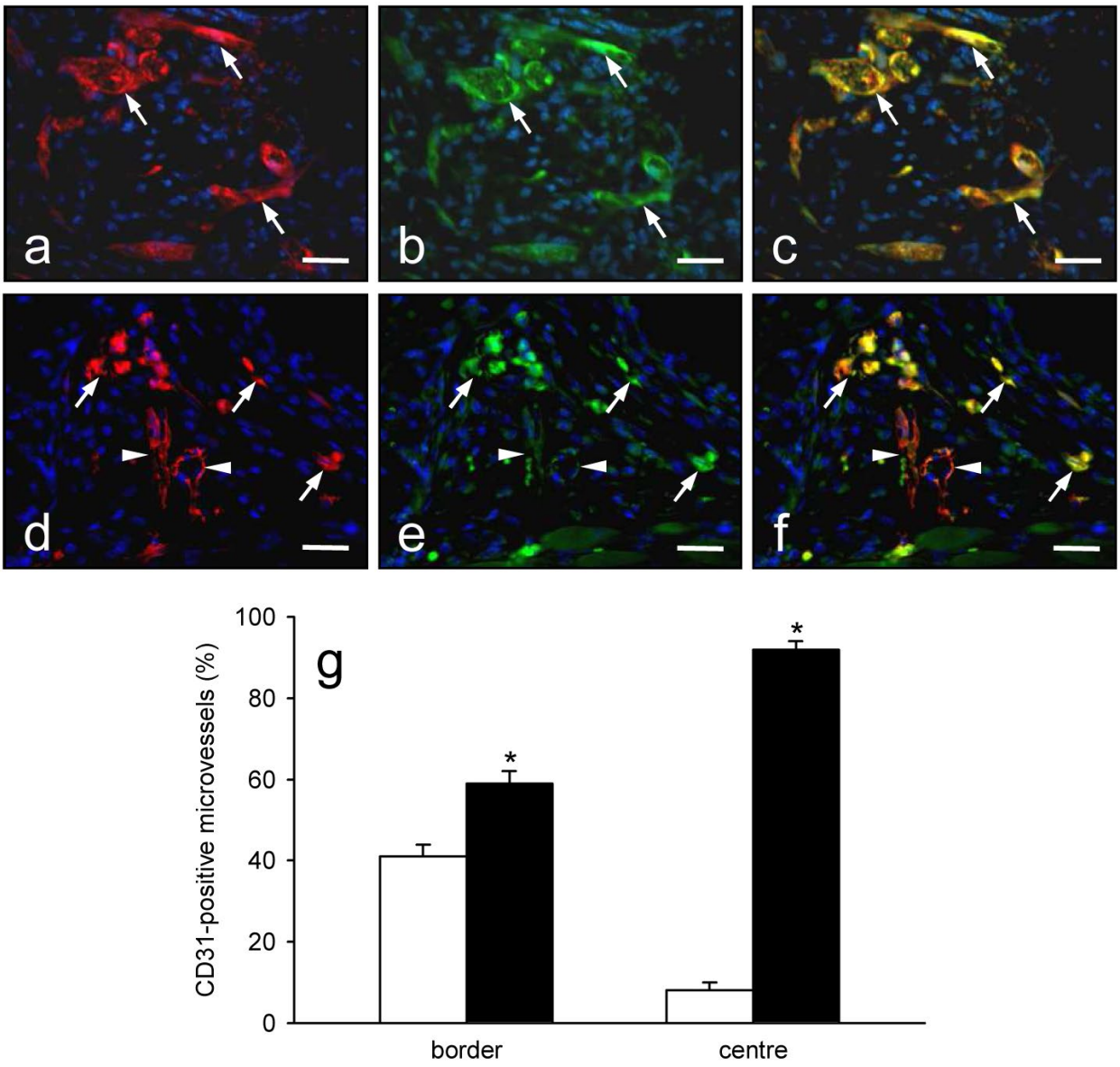

Fig. 5. a-f: Immunohistochemical characterisation of microvessels in the centre (a-c) and border (d-f) of a scaffold seeded with microvascular fragments at day 14 after implantation into the dorsal skinfold chamber. Histological sections were stained with bisbenzimide to identify cell nuclei (a-f, blue), an antibody against CD31 for the detection of endothelial cells (a, d, red) and an antibody against GFP (b, e, green). c and f display merges of a, b and d, e, respectively. Note that the microvessels in the centre (a-c, arrows) are double positive for CD31 and GFP. In the granulation tissue surrounding the scaffold, GFP-positive microvessels (d-f, arrows) growing out of the implant can be detected next to GFP-negative blood vessels of the host microvasculature (d-f, arrowheads). Scale bars: a-f = 36 µm. **g:** CD31-positive microvessels (%), which are GFP-positive (black bars) or GFP-negative (white bars), within the border and centre of scaffolds (n = 8) seeded with microvascular fragments at day 14 after implantation into dorsal skinfold chambers. Means ± SEM. *$p < 0.05$ *vs*. GFP-negative vessels.

affect their biocompatibility. However, in line with our intravital fluorescent microscopic results, they exhibited a markedly improved vascularisation, with a significantly increased microvessel density at the implants' border and centre zones (Figs. 4c-e).

Detailed immunohistochemical analyses of the microvascular networks in the group of scaffolds seeded with microvascular fragments showed that >90 % of all microvessels were GFP-positive in the centre of the implants at day 14 after implantation (Figs. 5a-c and g). This demonstrates that almost the entire microvasculature, contributing to the implants' internal blood supply, originated from GFP-positive microvascular fragments and was not replaced by ingrowing GFP-negative microvessels of the host. Moreover, ~60 % of microvessels in the granulation tissue surrounding the scaffolds were GFP-positive, indicating the growth of microvessels out of the implants into the host tissue (Figs. 5d-g).

Discussion

In tissue engineering, prevascularisation of tissue constructs represents a promising approach to guarantee their rapid and sufficient vascularisation after implantation into a host defect by the process of inosculation (Laschke *et al.*, 2009). In this context, we herein demonstrate that the vascularisation of implanted porous scaffolds is promoted by incorporation of adipose tissue-derived microvascular fragments. In fact, after their isolation these fragments are characterised by a good cell viability and a high capacity for forming functional microvascular networks within the implants. Thereby, they are capable of stimulating angiogenesis at the implantation site by the release of the pro-angiogenic growth factors VEGF and bFGF.

In contrast to common *in vitro* or *in situ* prevascularisation strategies, our novel approach bears the major advantage that fully functional microvessels can be seeded into porous scaffolds alone or in combination with stromal cells for the generation of tissue-specific constructs within a short time period of ~2 h. Accordingly, it does not involve complex cell cultivation procedures or repetitive surgical interventions. Adipose tissue represents an appealing source of microvascular fragments, because it can easily be harvested under clinical conditions by direct excision or minimally-invasive liposuction with low donor-site morbidity (Sterodimas *et al.*, 2010). Moreover, adipose tissue contains large numbers of mesenchymal stem cells, which have the ability to differentiate into adipogenic, chondrogenic, osteogenic, myogenic, neurogenic and endothelial lineages (Gimble *et al.*, 2007; Müller *et al.*, 2010; Witkowska-Zimny and Walenko, 2011). In line with this, we could demonstrate that isolated microvascular fragments contain many cells, which express the mesenchymal stem cell markers CD73 and CD117, as well as Sca-1/VEGFR-2-positive EPCs. This 'contamination' of the fragments with multipotent cells may further contribute to a high vascularisation and regenerative potential of the seeded scaffolds.

In the present proof-of-principle study, we seeded microvascular fragments onto porous nano-size hydroxyapatite particles/poly(ester-urethane) composite scaffolds. Recently, we could demonstrate that these scaffolds exhibit an excellent biocompatibility without inducing a strong inflammatory leukocytic host tissue response after implantation (Laschke *et al.*, 2010b). Due to their osteoconductive surface, these scaffolds may be particularly suitable for the tissue engineering of bone. However, the herein presented prevascularisation method with microvascular fragments may be transferable to any other three-dimensional porous scaffold type.

For this purpose, adequate seeding techniques are needed. In line with the current literature (Dai *et al.*, 2009), we found that the efficiency of static seeding by pipetting PBS containing microvascular fragments on top of our scaffolds was low, although the scaffolds exhibited large interconnected macropores of ~220 µm. Therefore, we established a dynamic seeding procedure during which negative and positive pressure could alternately be induced in the scaffold pores without complex technical equipment. By this, it was possible to remove the air out of the scaffold pores and, thus, to eliminate any surface tension produced by the air/PBS interface. In addition, the microvascular fragments could pass the scaffolds from both sides due to the changing pressure conditions, which contributed to their homogeneous distribution in the scaffold pores. Future studies have to clarify now, whether this rather simple procedure may also be effectively used in larger scaffolds and other scaffold types.

Using transgenic mice, we could analyse the fate of GFP-positive microvascular fragments, which were implanted for 14 d into the dorsal skinfold chamber of GFP-negative wild-type animals. Of interest, we found that the fragments were able to develop into GFP-positive microvascular networks, which inosculated with the GFP-negative host microvasculature of the implantation site. Recently, we reported that there are two basic modes of inosculation (Laschke *et al.*, 2009). Internal inosculation means that microvessels of the host invade a prevascularised tissue construct and develop interconnections to surviving preformed microvessels in the centre of the implant. On the other hand, preformed microvessels may grow out of a tissue construct into the surrounding host tissue, where external inosculation occurs. Based on the present results, we conclude that the blood perfusion of networks originating from isolated microvascular fragments is primarily established by external inosculation. In fact, >90 % of all microvessels in the centre of the scaffolds and ~60 % of microvessels in the surrounding host tissue were GFP-positive at day 14 after implantation. This indicates that the microvascular fragments survived throughout the implantation period and exhibited a high sprouting angiogenic activity.

The vascularisation of vessel-seeded scaffolds was associated with the formation of haemorrhages, which is a typical sign for extensive angiogenesis occurring inside the implants. In fact, one of the most important angiogenic factors, i.e. VEGF, is also a potent mediator of vascular permeability (Connolly, 1991). Thus, VEGF-mediated angiogenic processes promote haemorrhage formation (Jin Kim *et al.*, 2011). In line with these findings, in previous studies we have already detected haemorrhages in different types of scaffolds that exhibited a good vascularisation (Laschke *et al.*, 2008b; Laschke *et al.*, 2010a).

Although the vascularisation of our scaffolds could markedly be improved by seeding them with microvascular fragments, blood perfusion could not be detected in the centre of the implants until day 6. This is not a surprising finding, considering the fact that microvascular fragments first have to develop interconnections with each other and the host microvasculature to get fully reperfused. Accordingly, it will be necessary to establish novel strategies, which optimise the inosculation and vascularisation of seeded scaffolds, to avoid massive cell death in the centre of tissue-specific constructs during the very first days after implantation. This may be achieved by increasing the seeding density of microvascular fragments within the implants or by pre-cultivation of seeded

scaffolds in angiogenic media to stimulate the formation of functional microvascular networks prior to the implantation into a host defect.

In summary, we seeded in the present study for the first time porous scaffolds with microvascular fragments from adipose tissue. These fragments can easily be isolated within a short period of time and exhibit a high vascularisation potential, promoting the process of inosculation. Accordingly, this novel approach may markedly contribute to the rapid and sufficient vascularisation of tissue constructs and, thus, the success of future tissue engineering applications in clinical practice.

Acknowledgements

This work was supported by the Large Bone Defect Healing Program of AO Foundation. We are grateful for the excellent technical assistance of Janine Becker, Ruth M. Nickels and Julia Parakenings. We wish to confirm that there are no known conflicts of interest associated with this publication and there has been no significant financial support for this work that could have influenced its outcome.

References

Beier JP, Horch RE, Hess A, Arkudas A, Heinrich J, Loew J, Gulle H, Polykandriotis E, Bleiziffer O, Kneser U (2010) Axial vascularization of a large volume calcium phosphate ceramic bone substitute in the sheep AV loop model. J Tissue Eng Regen Med **4:** 216-223.

Beier JP, Hess A, Loew J, Heinrich J, Boos AM, Arkudas A, Polykandriotis E, Bleiziffer O, Horch RE, Kneser U (2011) *De novo* generation of an axially vascularized processed bovine cancellous-bone substitute in the sheep arteriovenous-loop model. Eur Surg Res **46:** 148-155.

Bramfeldt H, Sabra G, Centis V, Vermette P (2010) Scaffold vascularization: a challenge for three-dimensional tissue engineering. Curr Med Chem **17:** 3944-3967.

Connolly DT (1991) Vascular permeability factor: a unique regulator of blood vessel function. J Cell Biochem **47:** 219-223.

Dai W, Dong J, Chen G, Uemura T (2009) Application of low-pressure cell seeding system in tissue engineering. Biosci Trends **3:** 216-219.

Druecke D, Langer S, Lamme E, Pieper J, Ugarkovic M, Steinau HU, Homann HH (2004) Neovascularization of poly(ether ester) block-copolymer scaffolds *in vivo*: long-term investigations using intravital fluorescent microscopy. J Biomed Mater Res A **68:** 10-18.

Gimble JM, Katz AJ, Bunnell BA (2007) Adipose-derived stem cells for regenerative medicine. Circ Res **100:** 1249-1260.

Jin Kim Y, Hyun Kim C, Hwan Cheong J, Min Kim J (2011) Relationship between expression of vascular endothelial growth factor and intratumoral hemorrhage in human pituitary adenomas. Tumori **97:** 639-646.

Koike N, Fukumura D, Gralla O, Au P, Schechner JS, Jain RK (2004) Tissue engineering: creation of long-lasting blood vessels. Nature **428:** 138-139.

Kokemueller H, Spalthoff S, Nolff M, Tavassol F, Essig H, Stuehmer C, Bormann KH, Rücker M, Gellrich NC (2010) Prefabrication of vascularized bioartificial bone grafts *in vivo* for segmental mandibular reconstruction: experimental pilot study in sheep and first clinical application. Int J Oral Maxillofac Surg **39:** 379-387.

Laschke MW, Harder Y, Amon M, Martin I, Farhadi J, Ring A, Torio-Padron N, Schramm R, Rücker M, Junker D, Häufel JM, Carvalho C, Heberer M, Germann G, Vollmar B, Menger MD (2006) Angiogenesis in tissue engineering: breathing life into constructed tissue substitutes. Tissue Eng **12:** 2093-2104.

Laschke MW, Rücker M, Jensen G, Carvalho C, Mülhaupt R, Gellrich NC, Menger MD (2008a) Improvement of vascularization of PLGA scaffolds by inosculation of *in situ*-preformed functional blood vessels with the host microvasculature. Ann Surg **248:** 939-948.

Laschke MW, Rücker M, Jensen G, Carvalho C, Mülhaupt R, Gellrich NC, Menger MD (2008b) Incorporation of growth factor containing Matrigel promotes vascularization of porous PLGA scaffolds. J Biomed Mater Res A **85:** 397-407.

Laschke MW, Vollmar B, Menger MD (2009) Inosculation: connecting the life-sustaining pipelines. Tissue Eng Part B Rev **15:** 455-465.

Laschke MW, Mussawy H, Schuler S, Eglin D, Alini M, Menger MD (2010a) Promoting external inosculation of prevascularised tissue constructs by pre-cultivation in an angiogenic extracellular matrix. Eur Cell Mater **20:** 356-366.

Laschke MW, Strohe A, Menger MD, Alini M, Eglin D (2010b) *In vitro* and *in vivo* evaluation of a novel nanosize hydroxyapatite particles/poly(ester-urethane) composite scaffold for bone tissue engineering. Acta Biomater **6:** 2020-2027.

Laschke MW, Mussawy H, Schuler S, Kazakov A, Rücker M, Eglin D, Alini M, Menger MD (2011a) Short-term cultivation of *in situ* prevascularized tissue constructs accelerates inosculation of their preformed microvascular networks after implantation into the host tissue. Tissue Eng Part A **17:** 841-853.

Laschke MW, Vollmar B, Menger MD (2011b) The dorsal skinfold chamber: window into the dynamic interaction of biomaterials with their surrounding host tissue. Eur Cell Mater **22:** 147-164.

Levenberg S, Rouwkema J, Macdonald M, Garfein ES, Kohane DS, Darland DC, Marini R, van Blitterswijk CA, Mulligan RC, D'Amore PA, Langer R (2005) Engineering vascularized skeletal muscle tissue. Nat Biotechnol **23:** 879-884.

Lokmic Z, Stillaert F, Morrison WA, Thompson EW, Mitchell GM (2007) An arteriovenous loop in a protected space generates a permanent, highly vascular, tissue-engineered construct. FASEB J **21:** 511-522.

Lokmic Z, Mitchell GM (2008) Engineering the microcirculation. Tissue Eng Part B Rev **14:** 87-103.

Müller AM, Mehrkens A, Schäfer DJ, Jaquiery C, Güven S, Lehmicke M, Martinetti R, Farhadi I, Jakob M,

Scherberich A, Martin I (2010) Towards an intraoperative engineering of osteogenic and vasculogenic grafts from the stromal vascular fraction of human adipose tissue. Eur Cell Mater **19:** 127-135.

Novosel EC, Kleinhans C, Kluger PJ (2011) Vascularization is the key challenge in tissue engineering. Adv Drug Deliv Rev **63:** 300-311.

Okabe M, Ikawa M, Kominami K, Nakanishi T, Nishimune Y (1997) 'Green mice' as a source of ubiquitous green cells. FEBS Lett **407:** 313-319.

Shepherd BR, Chen HY, Smith CM, Gruionu G, Williams SK, Hoying JB (2004) Rapid perfusion and network remodeling in a microvascular construct after implantation. Arterioscler Thromb Vasc Biol **24:** 898-904.

Shepherd BR, Enis DR, Wang F, Suarez Y, Pober JS, Schechner JS (2006) Vascularization and engraftment of a human skin substitute using circulating progenitor cell-derived endothelial cells. FASEB J **20:** 1739-1741.

Shepherd BR, Hoying JB, Williams SK (2007) Microvascular transplantation after acute myocardial infarction. Tissue Eng **13:** 2871-2879.

Sterodimas A, de Faria J, Nicaretta B, Pitanguy I (2010) Tissue engineering with adipose-derived stem cells (ADSCs): current and future applications. J Plast Reconstr Aesthet Surg **63:** 1886-1892.

Wang ZZ, Au P, Chen T, Shao Y, Daheron LM, Bai H, Arzigian M, Fukumura D, Jain RK, Scadden DT (2007) Endothelial cells derived from human embryonic stem cells form durable blood vessels *in vivo*. Nat Biotechnol **25:** 317-318.

Warnke PH, Wiltfang J, Springer I, Acil Y, Bolte H, Kosmahl M, Russo PA, Sherry E, Lützen U, Wolfart S, Terheyden H (2006) Man as living bioreactor: fate of an exogenously prepared customized tissue-engineered mandible. Biomaterials **27:** 3163-3167.

Witkowska-Zimny M, Walenko K (2011) Stem cells from adipose tissue. Cell Mol Biol Lett **16:** 236-257.